2-13-2009

Efficient Gene Replacements in Toxoplasma gondii Strains Deficient for Nonhomologous End Joining

Barbara A. Fox
Dartmouth College

Jessica G. Ristuccia
Dartmouth College

Jason P. Gigley
Dartmouth College

David J. Bzik
Dartmouth College

EUKARYOTIC CELL, Apr. 2009, p. 520–529 Vol. 8, No. 4
1535-9778/09/$08.00+0 doi:10.1128/EC.00357-08

Efficient Gene Replacements in *Toxoplasma gondii* Strains Deficient for Nonhomologous End Joining▽†

Barbara A. Fox, Jessica G. Ristuccia, Jason P. Gigley,‡ and David J. Bzik*

Department of Microbiology and Immunology, Dartmouth Medical School, 1 Medical Center Drive, Lebanon, New Hampshire 03756

Received 31 October 2008/Accepted 2 February 2009

A high frequency of nonhomologous recombination has hampered gene targeting approaches in the model apicomplexan parasite *Toxoplasma gondii*. To address whether the nonhomologous end-joining (NHEJ) DNA repair pathway could be disrupted in this obligate intracellular parasite, putative KU proteins were identified and a predicted *KU80* gene was deleted. The efficiency of gene targeting via double-crossover homologous recombination at several genetic loci was found to be greater than 97% of the total transformants in *KU80* knockouts. Gene replacement efficiency was markedly increased (300- to 400-fold) in *KU80* knockouts compared to wild-type strains. Target DNA flanks of only ~500 bp were found to be sufficient for efficient gene replacements in *KU80* knockouts. *KU80* knockouts stably retained a normal growth rate in vitro and the high virulence phenotype of type I strains but exhibited an increased sensitivity to double-strand DNA breaks induced by treatment with phleomycin or γ-irradiation. Collectively, these results revealed that a significant KU-dependent NHEJ DNA repair pathway is present in *Toxoplasma gondii*. Integration essentially occurs only at the homologous targeted sites in the *KU80* knockout background, making this genetic background an efficient host for gene targeting to speed postgenome functional analysis and genetic dissection of parasite biology.

Toxoplasma gondii is a widespread obligate intracellular protozoan pathogen of virtually all warm-blooded animals and commonly infects humans worldwide. Due to a significant menu of established experimental approaches, *T. gondii* has become a model for the study of closely related disease-causing parasites (*Plasmodium*, *Theileria*, and *Cryptosporidium* species) belonging to the phylum *Apicomplexa* (32) and a model for the study of intracellular pathogens (33). Unfortunately, a high frequency of nonhomologous recombination arising from a previously undetermined double-strand break (DSB) DNA repair pathway(s) has hampered gene targeting approaches in this model.

DSB repair in most eukaryotes occurs primarily via two different recombination pathways (27). The homologous recombination pathways repair a DSB using mechanisms that recognize highly homologous DNA sequences, while the nonhomologous end-joining (NHEJ) pathway does not rely on DNA sequence homology. Instead, NHEJ involves direct ligation of the ends of broken DNA strands. KU70 and KU80 proteins form a heterodimer that tightly binds the DNA ends at the DSB, an early and essential step of NHEJ (49, 50). In addition to KU70 and KU80 proteins, NHEJ is mediated by the DNA ligase IV-Xrcc4 complex and the DNA-dependent protein kinase catalytic subunit or other functionally equivalent protein complexes (49).

Many eukaryotes preferentially use the NHEJ pathway to repair a DSB, and exogenous targeting DNA can be integrated anywhere into the genome independent of DNA sequence homology (27). The NHEJ pathway also appears to be preferentially used by *Toxoplasma gondii* based on the high rates of nonhomologous recombination and low gene targeting frequencies observed experimentally (7, 15, 26, 45). It is interesting that in contrast to the prevalence of the NHEJ pathway in eukaryotes, no functional NHEJ pathway has previously been reported in any protozoan parasite. Kinetoplastids, including *Trypanosoma* and *Leishmania* species, naturally exhibit extremely efficient homologous recombination of exogenous DNA (5, 12). While kinetoplastids possess the KU70 and KU80 components of the NHEJ pathway, recent evidence suggests that the NHEJ pathway is functionally absent (1, 24), although KU proteins do participate in telomere maintenance in *Trypanosoma brucei* (4, 30). *Plasmodium* species lack identifiable genes encoding key components of the NHEJ pathway and also exhibit a high frequency of homologous recombination (21, 51).

While most fungal organisms exhibit a low or modest gene targeting frequency, homologous recombination dominates at essentially a 100% frequency in *Saccharomyces cerevisiae* (22), making this budding yeast a significant model organism. Recent studies have reported that much higher frequencies of gene targeting are observed in mutants of *Aspergillus niger* (39), *Cryptococcus neoformans* (25), *Kluyveromyces lactis* (35), *Neurospora crassa* (29, 41), and other fungal organisms that have been engineered to be deficient in NHEJ. NHEJ-deficient fungal strains have greatly accelerated the development of genome-wide knockouts (3, 11).

* Corresponding author. Mailing address: Department of Microbiology and Immunology, Dartmouth Medical School, 1 Medical Center Drive, Lebanon, NH 03756. Phone: (603) 650-7951. Fax: (603) 650-6223. E-mail: david.j.bzik@dartmouth.edu.

† Supplemental material for this article may be found at http://ec.asm.org/.

‡ Present address: Department of Microbiology, Immunology, and Tropical Medicine, George Washington University Medical Center, Ross Hall, 2300 I Street, Washington, DC 20037.

▽ Published ahead of print on 13 February 2009.

TABLE 1. Strains used in this study

Strain	Parent	Genotype	Source or reference
RH	RH(ERP)	Wild type	44, 46
RHΔ*hxgprt*	RH	Δ*hxgprt*	6
RHΔ*ku80*::*HXGPRT*	RHΔ*hxgprt*	Δ*ku80*::*HXGPRT*	This study
RHΔ*hxgprt*Δ*ku80*::*DHFRTKTS*	RHΔ*ku80*::*HXGPRT*	Δ*hxgprt*Δ*ku80*::*DHFRTKTS*	This study
RHΔ*ku80*Δ*hxgprt*	RHΔ*ku80*::*HXGPRT*	Δ*ku80*Δ*hxgprt*	This study
RHΔ*ku80*	RHΔ*ku80*Δ*hxgprt*	Δ*ku80*	This study
RHΔ*ku80*Δ*uprt*::*HXGPRT*	RHΔ*ku80*Δ*hxgprt*	Δ*ku80*Δ*uprt*::*HXGPRT*	This study
RHΔ*ku80*Δ*uprt*Δ*hxgprt*	RHΔ*ku80*Δ*uprt*::*HXGPRT*	Δ*ku80*Δ*uprt*Δ*hxgprt*	This study
RHΔ*ku80*Δ*cpsII*::*CPSII*^{cDNA}*HXGPRT*	RHΔ*ku80*Δ*hxgprt*	Δ*ku80*Δ*cpsII*::*CPSII*^{cDNA}*HXGPRT*	This study

It was previously unknown whether a high frequency of nonhomologous recombination in *T. gondii* was due to KU-dependent NHEJ or arose from other potential mechanisms of DSB repair. In this report KU80 is found to be an essential component of a functional NHEJ pathway. *KU80* knockouts now allow the efficient targeting of gene replacements, gene knockouts, and gene "knock-ins" in *Toxoplasma gondii*.

MATERIALS AND METHODS

Primers. All oligonucleotide primers used in this study are listed in Table S1 in the supplemental material.

Plasmid constructs. Plasmids were based on pCR4-TOPO (Invitrogen), except for plasmid pC4HX1-1, which was based on a pET41 vector (20).

Plasmid pmin31-X2-4(-) was constructed from plasmid pminCAT/HX (6, 7), in which the *CAT* gene was replaced with the coding region for cytosine deaminase (*CD*) (14) (see Table S1 in the supplemental material).

Plasmid pΔKU80HXFCD was constructed by fusing, in order, a ~5.2-kb 5′ *KU80* target DNA flank from plasmid pAN442, the *HXGPRT* cassette (forward orientation) obtained from plasmid pmin31-X2-4(-), a 4.8-kb 3′ *KU80* target flank from plasmid pPN111, and a downstream *CD*-negative selectable marker (see Table S1 in the supplemental material). The 5′ and 3′ *KU80* target flanks in plasmid pΔKU80HXFCD surround a ~4-kb deletion of the *KU80* gene (2 kb 5′ untranslated region [UTR], exon 1, intron 1, and exon 2).

Plasmid pΔKU80B was based on plasmid pΔKU80HXFCD, in which the *HXGPRT* marker and part of the 5′ and 3′ target flanks were deleted by digestion with BamHI. Plasmid pΔKU80B contains 3.3-kb (5′) and 2.4-kb (3′) *KU80* target flanks that surround an ~8-kb deletion of the *KU80* gene (5′ UTR and all coding exons).

Plasmid pΔKU80TKFCD was based on plasmid pΔKU80HXFCD, in which NheI was used to further delete the *KU80* target flanks to 1.4 kb (5′) and 0.9 kb (3′) and join (forward orientation) the *DHFRTKTS* marker obtained from pDHFRTKTS (13).

Plasmid pΔUPNC was constructed by PCR to join a 1.1-kb *UPRT* 5′ target and a 0.67-kb 3′ *UPRT* target flank that surrounded a deletion of the *UPRT* coding region. The 5′ and 3′ *UPRT* target flanks in plasmid pΔUPNC surround a ~4.4-kb deletion of the *UPRT* gene that deletes 0.9 kb of 5′ UTR and the first six exons of *UPRT*.

Plasmid pΔUPT-HXB was constructed from plasmid pΔUPNC by inserting the *HXGPRT* marker in the forward orientation between the 5′ and 3′ *UPRT* target flanks. Plasmid pΔUPT-HXS was identical, except the 3′ *UPRT* target flank was 0.54 kb.

Plasmid pC4HX1-1 was constructed from plasmid pC4 (20), which contains the coding *CPSII* cDNA under the control of authentic *CPSII* 5′ and 3′ UTR, by adding the 1.95-kb *HXGPRT* marker in the forward orientation downstream of the *CPSII* 3′ UTR.

Plasmids of the pHXH-series were constructed by PCR (see Table S1 in the supplemental material), and products were cloned into pCR4-TOPO. Plasmids pHXH-0, pHXH-50, pHXH-120, pHXH-230, pHXH-450, pHXH-620, and pHXH-910 contained the 1.5-kb *HXGPRT* SalI fragment (containing the last 89 codons of *HXGPRT* plus 3′ UTR) surrounded by 0, ~50-bp flanks, ~120-bp flanks, ~230-bp flanks, ~450-bp flanks, ~620-bp flanks, and ~910-bp target DNA flanks, respectively. All pHXH series plasmids were oriented in the forward orientation relative to a unique PmeI site in pCR4-TOPO.

Strains and culture conditions. The parental strains of *Toxoplasma gondii* used in this study were RH (46) and RHΔ*hxgprt* (6). A list of strains used in this study is shown in Table 1. Parasites were maintained by serial passage in diploid human foreskin fibroblasts at 36°C (15).

Genomic DNA isolation and PCR. Genomic DNA purifications used the DNA Blood minikit (Qiagen). PCR products were amplified using a mixture (1:1) of *Taq* DNA polymerase and Expand long template PCR reagent (Roche). Real-time PCR used various concentrations of parasite DNA (1, 10, 100, 1,000, and 10,000 pg) amplified (in triplicate) with either the *T. gondii* B1 gene primer pairs B1F and B1R at 10 pM of each primer per reaction mixture (34) or using a primer pair specific to *KU80* (primers Ku80RTF and Ku80RTR). Amplification was performed by real-time fluorogenic PCR (Cepheid Smart Cycler) using one lyophilized SMartMix bead (SMartMix HM; Cepheid) per mixture. Each reaction mixture contained 1:20,000 SYBR Green I (Cambrex Bioscience). Parasite genome equivalents were determined by extrapolation from a standard curve using RHΔ*hxgprt* DNA.

Transformation of *Toxoplasma gondii* and knockout verification strategy. Electroporations (using a model BTX600 electroporator) were performed in 0.4 ml electroporation buffer containing 1.33×10^7 freshly isolated tachyzoites and 15 μg of DNA (10, 31). In gene replacement experiments the targeting plasmid was linearized 5′ of the 5′ target DNA flank. Following selection of parasite clones, the genotype of clones was determined by PCR to measure (i) loss of the deleted coding region of the targeted gene, (ii) correct targeted 5′ integration, (iii) correct targeted 3′ integration, and (iv) the presence of a target DNA flank. DNA sequence analysis and real-time PCR were also used for verification of knockouts.

***KU80* knockouts.** Strain RHΔ*ku80*::*HXGPRT* was constructed from RHΔ*hxgprt* by integration of the *HXGPRT* marker using plasmid pΔKU80HXFCD. Following transfection of tachyzoites with plasmid pΔKU80HXFCD, parasites were selected in mycophenolic acid (MPA; 25 μg/ml) and xanthine (50 μg/ml) (6). Negative selection experiments used flucytosine (5FC; 50 μM) (14). Parasite clones were isolated by limiting dilution (15). Verification of disruption of the *KU80* locus with the *HXGPRT* marker was performed by PCR with five sets of primers: PCR 1 used D801F and D801R, PCR 2 used EX801F and EX801R, PCR 3 used HXDF1 and HXDR2, PCR 4 used 80RTF and 80RTR, and PCR 5 used CDXF1 and CDXR2. The spontaneous reversion frequency of strain RHΔ*ku80*::*HXGPRT* was measured in 6-thioxanthine (6TX; 200 μg/ml) (43). Strain RHΔ*ku80*Δ*hxgprt* was constructed by targeted deletion of the *HXGPRT* marker using plasmid pΔKU80B and 6TX selection. Verification of removal of the *HXGPRT* marker from the *KU80* locus was performed by PCR with four sets of primers: PCR 2 used EX801F and EX801R, PCR 3 used HXDF1 and HXDR2, PCR 6 used EX80F2 and EX80R2, and PCR 7 used 80F15 and 80RCX3.

Determination of gene replacement frequencies and statistical analysis. PFU assays were used to determine absolute numbers of PFU that developed under different selection conditions, and then a formula was applied to calculate the gene replacement frequency (GRF) at the targeted locus. Four replicate PFU flasks were prepared for each titration point and each selection condition. A Student *t* test analysis was used to calculate the standard error of the mean.

Gene replacement at the *KU80* locus. Strain RHΔ*hxgprt*Δ*ku80*::*DHFRTKTS* was constructed from strain RHΔ*ku80*::*HXGPRT* by integration of the *DHFRTKTS* marker using plasmid pΔKU80TKFCD. Following transfection of tachyzoites with plasmid pΔKU80TKFCD, parasite clones were selected in pyrimethamine (PYR; 1 μM). Verification of replacement of the *HXGPRT* marker in the *KU80* locus with the *DHFRTKTS* marker was performed by PCR with six sets of primers: PCR 1 used HXDF1 and HXDR2, PCR 2 used EX80F2 and EX80R2, PCR 3 used EX80F3 and EX80R3, PCR 4 used TKXF1 and TKXR2, PCR 5 used CDXF1 and CDXR2, and PCR 6 used 80FCX3 and 80RCX3. PFU assays were performed at 15 days after transfection to determine the GRF based on the

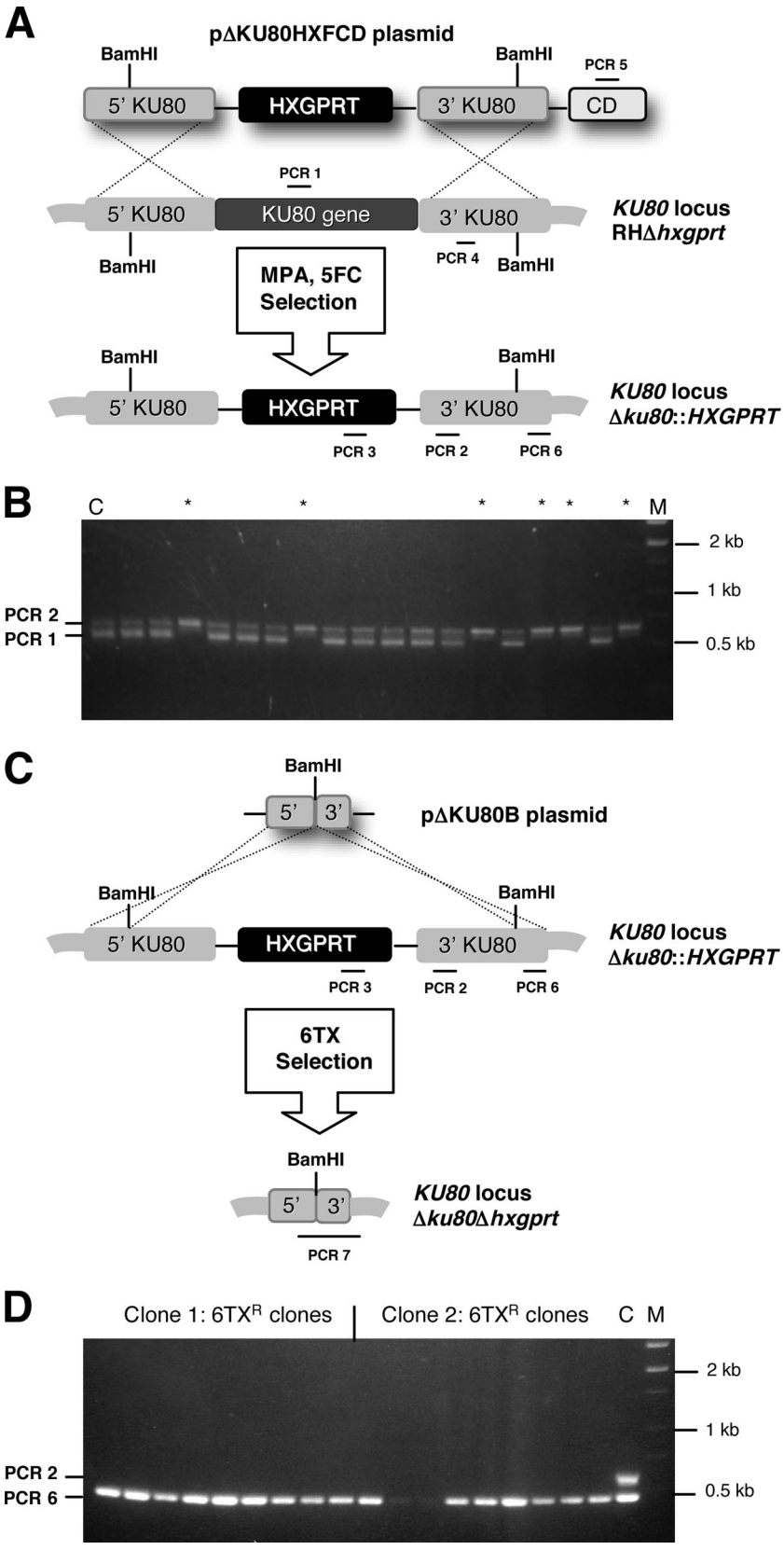

FIG. 1. Construction of *T. gondii* strains in which *KU80* is disrupted. (A) Strategy for disrupting the *KU80* gene via integration of the *HXGPRT* marker into strain RHΔ*hxgprt*. Targeting plasmid pΔKUHXFCD targets a ~4-kb deletion of the *KU80* gene (see Materials and Methods). Parasites were selected by positive selection in MPA plus xanthine or by negative selection against the downstream cytosine deaminase (*CD*) marker in MPA plus xanthine plus flucytosine.

fraction of parasites with dual resistance to PYR (1 μM) and 6TX compared to parasites with resistance only to PYR.

Gene replacement at the *UPRT* locus. Strain RHΔ*ku80*Δ*uprt*::*HXGPRT* was constructed from RHΔ*ku80*Δ*hxgprt* by targeted integration of the *HXGPRT* marker using plasmid pΔUPT-HXS or pΔUPT-HXB. Following transfection with plasmid pΔUPT-HXS or plasmid pΔUPT-HXB, parasites were selected in MPA and then cloned. Verification of disruption of the *UPRT* locus was performed by PCR with four sets of primers: PCR 1 used DUPRF1 and DUPRR1, PCR 2 used UPNF1 and UPNXR1, PCR 3 used 3′DHFRCXF and 3′CXP MUPR15′, and PCR 4 used 5′UPNCXF and 5′DHFRCXR. PFU assays were performed at various times after transfection to determine the GRF based on the fraction of parasites that had dual resistance to MPA and 5-fluorodeoxyuridine (FUDR; 5 μM) compared to the fraction of parasites that were resistant only to MPA. Strain RHΔ*ku80*Δ*uprt*Δ*hxgprt* was constructed by targeted deletion of the *HXGPRT* marker using plasmid pΔUPNC. Following transfection with plasmid pΔUPNC, parasites were continuously selected in 6TX. Validation PCRs used primer pairs 3′DHFRCXF with 3′CXPMUPR1 and CLUPF1 with 3′CXP-MUPR1.

Gene replacement at the *CPSII* locus. Strain RHΔ*ku80*Δ*cpsII*::*CPSII*^{cDNA} *HXGPRT* was constructed from RHΔ*ku80*Δ*hxgprt* by integration of the *HXGPRT* marker using plasmid pC4HX1-1. Verification of deletion of the endogenous *CPSII* locus and replacement with a functional *CPSII* cDNA was performed by PCR with four sets of primers: PCR 1 used CPSDF1 and CPSDR1, PCR 2 used CPSEXF1 and CPSEXR1, PCR 3 used CPSCXF1 and CPSCXR1, and PCR 4 used 3′DHFRCXF and CPSCXR2.

Chromosomal repair of Δ*hxgprt*. Strain RHΔ*ku80* was constructed from RHΔ*ku80*Δ*hxgprt* by repair of the Δ*hxgprt* chromosomal locus using pHXH plasmids with various lengths of homologous DNA that flanked a 1.5-kb SalI fragment which had been deleted in the Δ*hxgprt* background (6). Verification of chromosomal repair of *HXGPRT* was performed by PCR with primers HXF1200 and HXDR2. The frequency of chromosomal repair events at the *HXGPRT* locus was determined in PFU assays in a single 150-cm^2 flask of human foreskin fibroblast cells with MPA selection following transfection. Each pHXH series plasmid was transfected in five independent repair experiments, and the mean PFU was determined. The percent maximal homologous recombination at the *HXGPRT* locus was then calculated based on comparison to results from the pHXH-910 plasmid, which carried the longest target DNA flanks. The fraction of tachyzoites surviving transfection was measured in each transfection experiment in a PFU assay. Plasmid pHXH-620 was used to determine the percent maximal homologous recombination as a function of DNA concentration or conformation.

Parasite growth rate. Tachyzoite growth rate was determined by scoring 50 randomly selected vacuoles as previously described (15).

Sensitivity to chemical mutagens and phleomycin. Sensitivity to *N*-nitroso-*N*-ethylurea (ENU; Sigma) was determined by treatment of replicating intracellular parasites using previously described methods (44). Etoposide (Sigma) sensitivity was determined by continuous treatment of infected monolayers in PFU assays as previously described (47). Sensitivity to the antibiotic phleomycin (Sigma) was determined on extracellular parasites as previously described (38), except PFU assays were used rather than uracil incorporation to measure viability. Parasite viability experiments with ENU, etoposide, and phleomycin were performed twice.

Sensitivity to γ-irradiation. Sensitivity to γ-irradiation was determined by treatment of tachyzoites with various doses of ionizing radiation that were generated in a 2,000-Ci JL Shepard cesium (Cs137 gamma) irradiator. PFU assays were used to determine the surviving fraction of treated parasites relative to untreated controls. Parasite survival experiments involving γ-irradiation were performed twice.

Virulence assays. Adult 6- to 8-week-old C57BL/6 mice were obtained from Jackson Labs and mice were maintained in Tecniplast Seal Safe mouse cages on vent racks at the Dartmouth-Hitchcock Medical Center (Lebanon, NH) mouse facility. All mice were cared for and handled according to the Animal Care and Use Program of Dartmouth College using National Institutes of Health-approved institutional animal care and use committee guidelines. Groups of four mice were injected intraperitoneally with 0.2 ml (200 tachyzoites) and mice were then monitored daily for degree of illness and survival. Virulence assays were performed twice.

RESULTS

Generation of *T. gondii* strains RHΔ*ku80*::*HXGPRT* and RHΔ*ku80*Δ*hxgprt*. To look for potential components of the NHEJ pathway in *T. gondii* the ToxoDB genome database (http://www.toxodb.org/toxo/; release 3.0) was scanned for potential KU70 and KU80 proteins. BLASTp analysis of the KU70 (*mus51*) and KU80 (*mus52*) proteins of *Neurospora crassa* identified *T. gondii* homologs encoded by genes at loci 50.m03211 and 583.m05492, respectively (alignments are shown in Fig. S1 and Fig. S2 in the supplemental material).

Circular or linearized plasmid pΔKU80HXFCD was transfected into strain RHΔ*hxgprt* and parasites were selected in MPA (Fig. 1A). Transfection with circular plasmids produced no *KU80* knockouts (0/36 [data not shown]), while transfections with linearized plasmids produced 11/36 clones that showed a correct PCR 2 product but no detectable PCR 1 product that corresponded to the deleted region and identified *KU80*-disrupted clones (Fig. 1B). Real-time PCR analysis (PCR 4) of *KU80* gene copy number indicated that ~82% of the *KU80*-disrupted clones contained a single copy of the *KU80* 3′ target DNA (Fig. 1A and B). In *KU80*-disrupted clones, PCR 3 was positive (presence of *HXGPRT* marker) and PCR 5 was negative (absence of the *CD* marker) (data not shown). These results suggested that the *HXGPRT* marker was inserted into a correctly disrupted *KU80* locus (Fig. 1B).

A downstream *CD* marker on plasmid pΔKU80HXFCD was tested in a negative selection strategy using 5FC to enrich for the desired *KU80* knockouts (Fig. 1A). Transfected parasites were initially selected in MPA for 10 days, then were cloned in MPA plus 5FC to counterselect against the downstream *CD* gene (Fig. 1A). We observed that six of six analyzed clones were *KU80* knockouts (data not shown).

To recover the *HXGPRT* marker from the *KU80* locus, clones of strain RHΔ*ku80*::*HXGPRT* were transfected with plasmid pΔKU80B (Fig. 1C) and nine 6TX-resistant clones were obtained from each transfection. Each 6TX-resistant clone had the genotype Δ*ku80*Δ*hxgprt* (Fig. 1D), based on the presence of correct product from PCR 6 and the absence of any product from PCR 2 (Fig. 1C and D). PCR 3 also revealed the expected loss of the *HXGPRT* marker, and PCR 7 produced a correct product (~2.9 kb) showing targeted integration of the 3′ target DNA flank (data not shown).

Approximate locations of PCR products using primer pairs to verify genotype are depicted (not to scale). The parental strain RHΔ*hxgprt* was positive for PCR 1 (538-bp product) and PCR 2 (639-bp product). A targeted *KU80* knockout was positive for the PCR 2 product and was negative for the PCR 1 product. (B) A representative panel of 18 MPA-resistant clones obtained after transfection of plasmid pΔKU80HXFCD and selection in MPA. Clones marked with a * show a pattern consistent with targeted deletion of a region of the *KU80* gene (see text). (C) Cleanup of the *KU80* locus. The *HXGPRT* marker was removed from the *KU80* locus using the strategy depicted with negative selection in 6TX after transfection of strain RHΔ*ku80*::*HXGPRT* with plasmid pΔKU80B. Approximate locations of PCR products using primer pairs to verify genotype are depicted (not to scale). The parental strain RHΔ*ku80*::*HXGPRT* was positive for PCR 2 (639-bp product) and PCR 6 (373-bp product) and a plasmid pΔKU80B-retargeted *KU80* knockout was positive for PCR 6 and was negative for PCR 2. (D) 6TX-resistant clones uniformly had the genotype Δ*ku80* Δ*hxgprt*.

Growth, virulence, and sensitivity of *T. gondii* strains RHΔ*hxgprt*, RHΔ*ku80*::*HXGPRT*, and RHΔ*ku80*Δ*hxgprt* to DNA damaging agents. Disruption of *KU70* or *KU80* typically induces an increased sensitivity to DNA damaging agents, particularly to agents that cause double-strand DNA breaks (25, 35, 39). Tachyzoite growth rate, sensitivity to ENU, and sensitivity to etoposide were unchanged between strains RHΔ*ku80*::*HXGPRT* and RHΔ*ku80*Δ*hxgprt* compared to RHΔ*hxgprt* or RH (data not shown). The higher virulence of type I strains was also retained in the *KU80* knockout mutants (Fig. 2A). In contrast, phleomycin treatments of 5 μg/ml or 50 μg/ml reduced parental RHΔ*hxgprt* viability to 56% (±16%) and 2.1% (0.9%), reduced strain RHΔ*ku80*::*HXGPRT* viability to 19% (±8%) and 0.19% (±0.05%), and reduced strain RHΔ*ku80*Δ*hxgprt* viability to 14% (±3%) and 0.23% (±0.02%), respectively (Fig. 2B). *KU80* knockouts were 2.9- to 4.0-fold more sensitive to 5 μg/ml and 9- to 11-fold more sensitive to 50 μg/ml phleomycin treatment than the parental strains. Sensitivity to γ-irradiation was also significantly increased in *KU80* knockouts. At a dose of 35 Gy, the percent parasite viability of strain RHΔ*hxgprt* was 5.4% (±1.1%), viability of strain RHΔ*ku80*::*HXGPRT* was 0.013% (±0.005%), and viability of strain RHΔ*ku80*Δ*hxgprt* was 0.010% (±0.003%) (Fig. 2C). *KU80* knockouts were between 415- and 540-fold more sensitive to γ-irradiation (35-Gy dose) than the parental strains.

GRF at the *KU80* locus. A simple PFU assay strategy was devised to measure the percentage of gene replacement events at the disrupted *KU80* locus. This strategy (see Materials and Methods) targeted the replacement of the *HXGPRT* gene (inserted at the *KU80* locus in strain RHΔ*ku80*::*HXGPRT*) with the trifunctional *DHFRTKTS* gene. Using target DNA flanks of only 1.3 and 0.9 kb carried on targeting plasmid pΔKU80TKFCD, the efficiency of gene replacement at the *KU80* locus was 97.1% (±2.3%) (data not shown).

GRF at the uracil phosphoribosyltransferase locus. To measure gene replacement efficiency in *KU80* knockouts compared to parental strains, we targeted the disruption of the *UPRT* locus. Loss of uracil phosphoribosyltransferase (UPRT) function in any genetic background results in resistance to FUDR (7, 9, 42). A fixed 5′ target DNA flank of 1.3 kb and either a 0.54-kb (plasmid pΔUPT-HXS [not shown]) or a 0.67-kb (plasmid pΔUPT-HXB) 3′ target DNA flank were used in the *UPRT* disruption assay (Fig. 3A). The frequency of gene replacement (*UPRT* knockout) was determined at different time points after transfection by plating equal numbers of parasites in either MPA or MPA plus FUDR selection (Fig. 3B). The frequency of gene replacement at the *UPRT* locus in strain RHΔ*ku80*Δ*hxgprt* was 99.8% (±0.6%) when assayed at 20 days posttransfection (Table 2). Similar results were observed using plasmid pΔUPT-HXS (data not shown). The comparative gene replacement percent efficiency in the parental strain RHΔ*hxgprt* was 0.30% (±0.04%). The relative efficiency of gene replacement was enhanced by 300- to 400-fold at the *UPRT* locus in strain RHΔ*ku80*Δ*hxgprt* compared to the efficiency measured in the parental strain RHΔ*hxgprt*.

The nonreverting genotype Δ*ku80* Δ*uprt*::*HXGPRT* was confirmed in several MPA-resistant clones (Fig. 3C). A cleanup vector, pΔUPNC, containing 5′ and 3′ *UPRT* target DNA flanks but no *HXGPRT* marker, was then used to target the removal of the integrated *HXGPRT* marker from the *UPRT* locus in a clone of strain RHΔ*ku80*Δ*uprt*::*HXGPRT* to generate strain RHΔ*ku80*Δ*uprt*Δ*hxgprt* (data not shown).

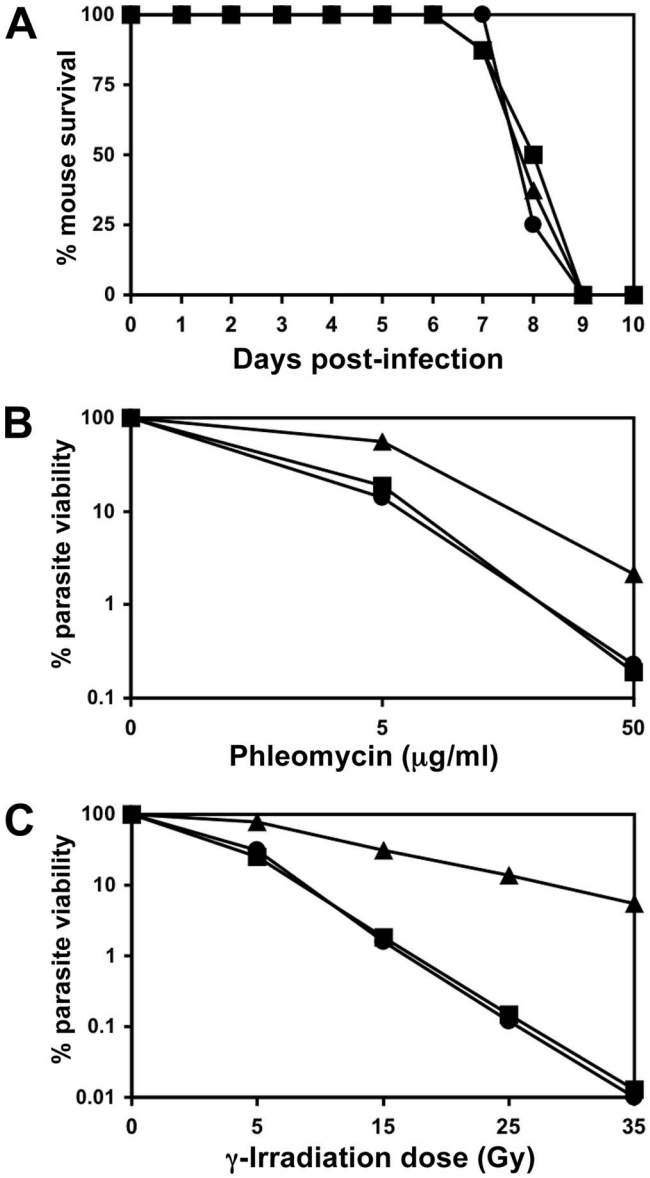

FIG. 2. Phenotypes of *KU80* knockout strains. (A) Virulence of strains was determined by intraperitoneal infection of C57BL/6 mice with 200 tachyzoites. Results of a representative experiment (of two experiments) in which groups of four mice were infected with freshly isolated tachyzoites from strain RHΔ*hxgprt* (triangles), strain RHΔ*ku80*::*HXGPRT* (circles), or strain RHΔ*ku80*Δ*hxgprt* (squares). (B) Sensitivity of extracellular tachyzoites to phleomycin. Strains RHΔ*hxgprt* (triangles), RHΔ*ku80*::*HXGPRT* (circles), or RHΔ*ku80*Δ*hxgprt* (squares) were treated with phleomycin (two replicate experiments; see text), and survival was determined relative to untreated controls. Results of a representative experiment are shown. (C) Sensitivity of extracellular tachyzoites to γ-irradiation. Strains RHΔ*hxgprt* (triangles), RHΔ*ku80*::*HXGPRT* (circles), and RHΔ*ku80*Δ*hxgprt* (squares) were treated with γ-irradiation (two replicate experiments; see text), and survival was determined relative to untreated controls. Results of a representative experiment are shown.

Gene replacement at the carbamoyl phosphate synthetase II (CPSII) locus. Our previous work revealed a very low (~0.2%) frequency of gene targeting at the essential *CPSII* locus (15).

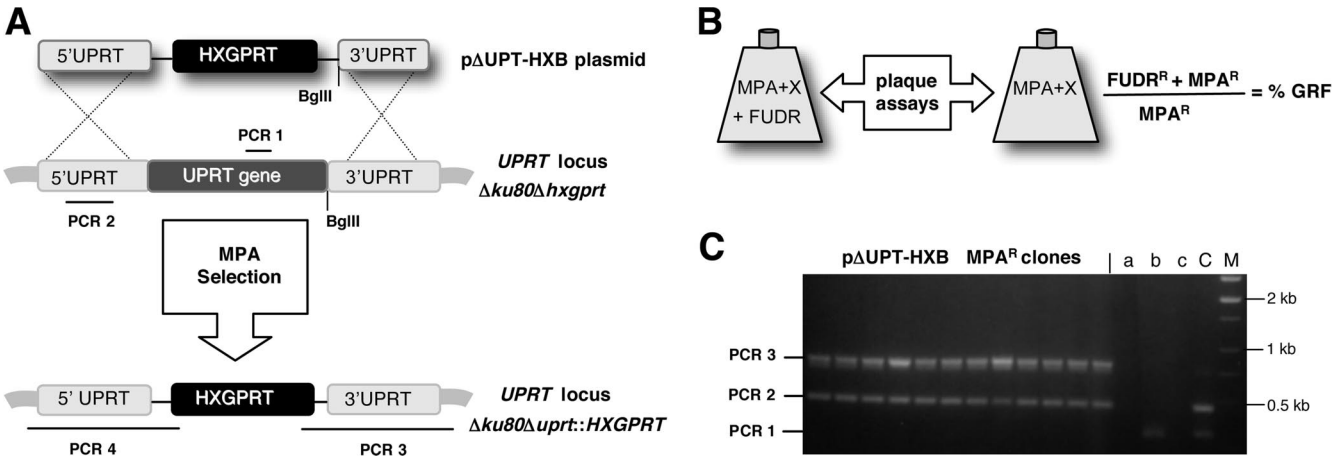

FIG. 3. Targeted gene replacement at the uracil phosphoribosyltransferase (*UPRT*) locus. (A) Strategy for disruption of *UPRT* by a double-crossover homologous recombination event in strain RHΔ*hxgprt* or RHΔ*ku80*Δ*hxgprt* by using a fixed 5′ target flank of 1.3 kb and a 3′ target DNA flank of 0.67 kb on plasmid pΔUPT-HXB. The PCR strategy for genotype verification is depicted using primer pairs to assay for products from the PCR (not to scale). (B) PFU assays were performed at various times after transfection to determine the GRF based on the fraction of parasites that had dual resistance to MPA and FUDR (5 μM) compared to the fraction of parasites that were resistant to MPA (Table 2). (C) Genotype verification of clones selected for MPA resistance after transfection with the pΔUPT-HXB plasmid. For parental strain RHΔ*hxgprt*, PCR 1 was positive (304-bp product; lane b), PCR 2 was positive (460-bp product; lane C), and PCR 3 was negative (840-bp product; lane a). For MPA-resistant clones isolated after transfection with plasmid pΔUPT-HXB, PCR 1 was negative, PCR 2 was positive, and PCR 3 was positive. Control lane (c) contained no template and the PCR 1 and PCR 2 primers. Twelve of 12 MPA-resistant clones revealed targeted gene replacement at the *UPRT* locus.

Gene replacement efficiency at the *CPSII* locus was examined in strain RHΔ*ku80*Δ*hxgprt* using a direct replacement knock-in strategy (Fig. 4A). Target flanks of 1.5 kb 5′ and 0.8 kb 3′ that surrounded the *CPSII* cDNA minigene and an *HXGPRT* marker (plasmid pC4HX1-1) were used to delete the endogenous *CPSII* gene and replace it with a functional *CPSII* cDNA (*CPSII*^{cDNA}) (20). Each MPA-resistant clone failed to produce any PCR 1 product specific to intron 27 of the endogenous *CPSII* locus and using primers positioned within exons 21 and exon 23 (PCR 2) produced a PCR product that corresponded to targeting cDNA rather than originating from the endogenous *CPSII* locus (Fig. 4A and B). These results indicated that gene replacement had uniformly occurred at the *CPSII* locus in strain RHΔ*ku80*Δ*hxgprt*. Sequencing of correctly sized PCR 3 and PCR 4 products (data not shown) verified the genotype of this strain as Δ*ku80*Δ*cpsII*::*CPSII*^{cDNA}*HXGPRT* (Fig. 4 and Table 1).

Parameters affecting the efficiency of gene targeting in *KU80* knockouts. In fungal strains deficient for NHEJ the overall gene targeting efficiency is increased due to a marked reduction in the frequency of nonhomologous recombination, rather than to any significant increase in the efficiency of homologous recombination (25, 35, 39, 41). To verify that loss of nonhomologous recombination is the explanation behind increased gene targeting efficiency in *KU80* knockouts versus the alternative mechanism, that homologous recombination efficiency is increased, we devised a novel strategy to specifically and quantitatively measure homologous recombination (only double-crossover events) in Δ*hxgprt* genetic backgrounds of both the Δ*ku80* and the parental strain. As shown in Fig. 5A, this strategy targets the repair of a disrupted Δ*hxgprt* locus. The output of each targeted repair event is a single MPA-resistant PFU (see Materials and Methods). No PFU can arise from any nonhomologous recombination event (even if they occur), because each targeting plasmid carries only a fragment of the *HXGPRT* gene that cannot confer MPA resistance in the Δ*hxgprt* background. Double-crossover homologous recombination mediated by targeting DNA flank lengths of 0, 50, 120, 230, 450, 620, and 910 bp was examined. At each target DNA flank length (except 230 bp) the efficiency of gene replacement via double-crossover homologous recombination at the *HXGPRT* locus was similar (within twofold on a per parasite basis [data not shown]) between strain RHΔ*ku80*Δ*hxgprt* and the parental strain, RHΔ*hxgprt* (Fig. 5B). These results, along with data shown in Fig. 2, 3, and 4 and Table 2, reveal that the increased gene targeting efficiency in *KU80* knockouts arises from the loss of a major nonhomologous recombination pathway rather than from any significant increase in the efficiency of homologous recombination.

TABLE 2. GRFs at the *UPRT* locus

Strain	Plasmid	Day assayed	% Gene replacement at *UPRT* locus	
			Expt 1	Expt 2
RHΔ*hxgprt*	pΔUPT-HXB	10	0.26	0.20
RHΔ*hxgprt*	pΔUPT-HXB	14	0.31	0.29
RHΔ*hxgprt*	pΔUPT-HXB	20	0.33	0.26
RHΔ*ku80*Δ*hxgprt*	pΔUPT-HXB	10	82.8	90.0
RHΔ*ku80*Δ*hxgprt*	pΔUPT-HXB	14	97.1	96.3
RHΔ*ku80*Δ*hxgprt*	pΔUPT-HXB	20	99.2	100.4

The minimal target DNA flank length for gene replacement at the *HXGPRT* locus was determined (Fig. 5B). No gene replacement events were detected in strain RHΔ*hxgprt* when we used 230-bp target DNA flanks. While strain RHΔ*ku80*Δ*hxgprt* exhibited a detectable frequency of gene replacement using 230-bp

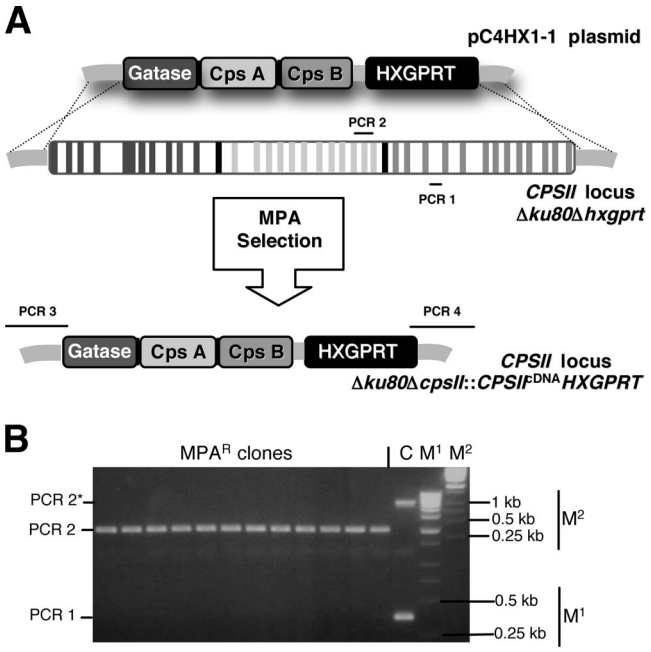

FIG. 4. Targeted gene replacement at the carbamoyl phosphate synthetase II (*CPSII*) locus. (A) Strategy for deletion of ~24 kb of the endogenous *CPSII* locus by using a functional *CPSII* cDNA minigene and a downstream *HXGPRT* marker flanked by a 1.5-kb 5′ target and a 0.8-kb 3′ target. The 37 exons (shaded rectangles) and 36 introns (white rectangles) of the endogenous *CPSII* locus are shown (not to scale). PCR primer pairs (PCRs 1 to 4; see Materials and Methods) were used to amplify PCR products to verify genotype (not to scale). In strains RHΔ*hxgprt* and RHΔ*ku80*Δ*hxgprt* the expected PCR product size from PCR 1 was 382 bp and from PCR 2* was 1,084 bp. If targeted replacement occurred at the *CPSII* locus, the expected PCR 2 product would be 363 bp, and no product was produced from PCR 1 because the targeting plasmid *CPSII* cDNA does not contain the PCR 1 primer sites located in intron 27 (see panel A above). (B) Twelve of 12 MPA-resistant clones revealed targeted gene replacement occurred at the *CPSII* locus in strain RHΔ*ku80*Δ*hxgprt*. To more clearly visualize PCR products those from PCR 1 were resolved for ~45 min using the markers in lane M^1, and then the same agarose gel was reloaded with PCR products from PCR 2 and using markers in lane M^2 for the control. Control lane C shows the products from PCR 1 (382-bp product) and PCR 2* (1,084-bp product) using parental RHΔ*ku80*Δ*hxgprt* template DNA (endogenous *CPSII* locus).

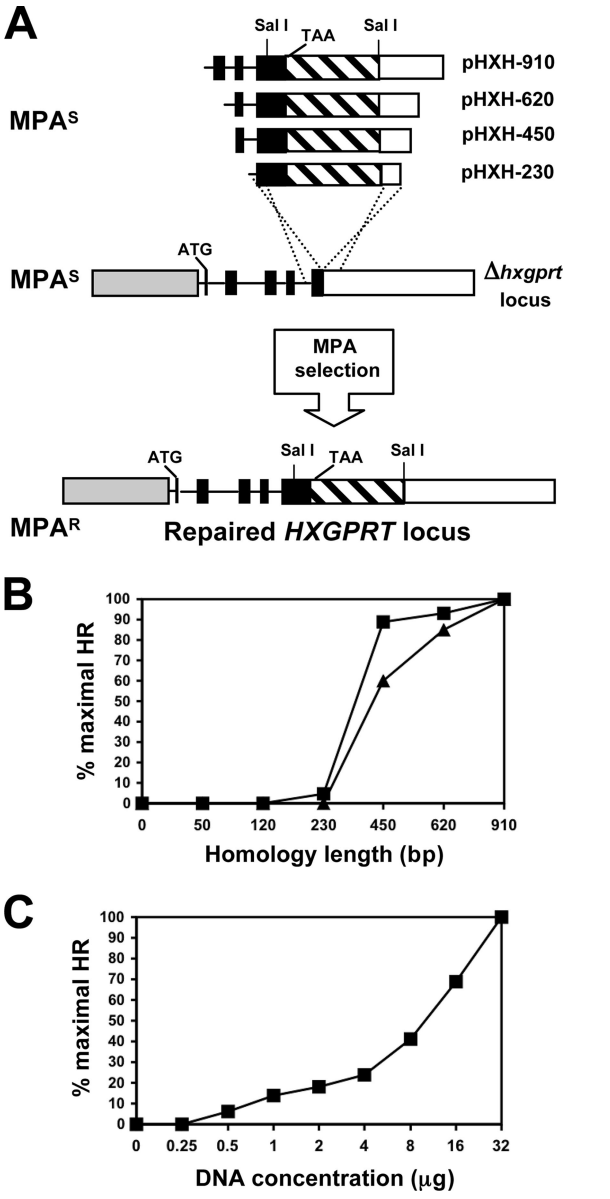

FIG. 5. *KU80* knockouts efficiently target gene replacements due to a deficiency in nonhomologous recombination. (A) Strategy for targeted repair of the Δ*hxgprt* locus using different lengths of flanking target DNA that surround a 1.5-kb SalI fragment that is deleted in the Δ*hxgprt* background (see text). (Top) Targeting plasmids with 230-, 450-, 620-, and 910-bp target DNA flanks are shown. Plasmids with 120-bp, 50-bp, or 0-bp targeting DNA flanks are not shown. All pHXH targeting plasmids are MPA sensitive (MPA^s). The termination codon (TAA) of the *HXGPRT* gene is shown. (Middle) The structure of the Δ*hxgprt* locus for MPA^s strains RHΔ*hxgprt* and RHΔ*ku80*Δ*hxgprt* is shown. The gene structure is depicted by exons (dark rectangles), introns (lines), a 5′ UTR (gray rectangle), 3′ UTR (rectangular box with diagonal lines), and a far downstream 3′ UTR (open rectangle). The disrupted locus contains an intact 5′ UTR, intact exon 1 (ATG start is shown) to exon 4, and the deletion in exon 5 and the 3′ UTR contained in the missing 1.5-kb SalI fragment. A hypothetical double-crossover homologous recombination gene targeting event is shown by the dotted lines linking the targeting pHXH plasmids. (Bottom) MPA-resistant (MPA^r) parasites can only arise by the double-crossover homologous recombination gene targeting event shown. (B) The percent maximal homologous recombination was determined in strain RHΔ*hxgprt* (triangles) and strain RHΔ*ku80*Δ*hxgprt* (squares) (see Materials and Methods). (C) The percent maximal homologous recombination was determined as a function of targeting DNA concentration.

target DNA flanks, the overall efficiency was reduced by 22-fold compared to target DNA flanks of 450 bp or more (Fig. 5B). No gene replacement events were detected using target DNA flanks of 120 bp or less in any strain.

The efficiency of gene replacement at the *HXGPRT* locus was dependent on targeting DNA concentration (Fig. 5C). No gene replacement events were detected at the *HXGPRT* locus using circular targeting DNA in strain RHΔ*hxgprt*. In contrast, a detectable frequency was observed in strain RHΔ*ku80*Δ*hxgprt*, although the efficiency of gene replacement was reduced by 20-fold compared to linearized targeting DNA.

DISCUSSION

A nonreverting gene knockout at the *KU80* locus functionally disrupts the NHEJ DSB DNA repair pathway in *T. gondii*.

Due to disruption of nonhomologous recombination mediated by the NHEJ pathway, *KU80* knockouts exhibit a markedly higher gene replacement efficiency compared to wild-type strains. Our results suggest that disruption of *KU80* leads to a nearly complete disruption of all nonhomologous recombination-mediated DSB DNA repair pathways in *T. gondii*. To our knowledge, this is the first report that clearly demonstrates the existence of a functional and significant KU-dependent NHEJ pathway in a protozoan parasite.

Readily identifiable *KU* genes are notably absent in *Plasmodium* species (http://plasmodb.org/plasmo; release 5). KU proteins are present but they do not participate in NHEJ in other protozoans such as *Leishmania* and *Trypanosoma* species (1, 24). It is puzzling that while NHEJ is prevalent in eukaryotes, a functional NHEJ pathway has not been previously described in protozoa. We speculate that acquisition and retention of a functional NHEJ DSB DNA repair pathway in *T. gondii* may correlate with the presence of extracellular developmental stages that occur in the oocyst. The oocyst stage must maintain viability through development and maintenance of sporocysts and sporozoites under harsh environmental conditions in soil and water for a long period of time prior to their successful transmission to intermediate hosts via oral ingestion.

The mechanisms of NHEJ had not been previously dissected in *T. gondii*. Our results show KU80 to be an essential component of the NHEJ mechanism in *T. gondii*. The *Toxoplasma gondii* genome (http://beta.toxodb.org/toxo5.0/) also reveals genes encoding putative DNA ligase IV (TGGT1_073840) and DNA-dependent protein kinase (57.m01765) components of eukaryotic NHEJ. Similar to other described proteins from parasites in the phylum *Apicomplexa* (16, 19), the predicted KU70 and KU80 proteins are markedly enlarged compared to other species of known KU proteins. Before initiating our studies at the *KU80* gene, we targeted knockouts directed at both the *KU70* gene and the *DNA ligase IV* gene, and these knockout attempts were not successful in strain RHΔ*hxgprt*. Subsequent attempts to disrupt *KU70* and the *DNA ligase IV* gene in the RHΔ*ku80*Δ*hxgprt* background were also unsuccessful. Our negative results at these two loci suggest that these genes encode essential functions, or that their loci are refractory to gene targeting (data not shown).

KU80 knockouts retain a normal tachyzoite growth rate as well as high virulence typical of type I strains in murine infection. *KU80* knockouts are highly stable in culture and have shown no fluctuation in growth rate, virulence, or the enhanced gene targeting phenotype after continuous passage for more than 1,600 generations. *KU80* knockouts do exhibit an increased sensitivity to double-strand DNA breaks induced by phleomycin or γ-irradiation. No other major cellular or developmental defects have been noted so far in most fungal organisms disrupted in NHEJ (25, 35, 39, 41).

We find circular DNA to be a particularly poor substrate for double-crossover homologous recombination necessary for gene replacement in *T. gondii*. This conclusion is also supported by previous evidence (8). We find that DNA target flanks of 120 bp or less do not produce detectable gene replacements at the *HXGPRT* locus. Using targeting strategies directed at the *UPRT*, *CPSII*, *KU80*, and *HXGPRT* loci, we showed that efficient gene targeting now occurs in *KU80* knockouts using target DNA flanks of ~500 bp or greater.

Recently, downstream markers such as *UPRT*, *HXGPRT*, or *YFP* have been used to enrich selected populations for desired double gene replacement events (23, 36, 37). Our results validate the use of the *CD* marker outside of the targeting cassette as another potent strategy to enrich for desired gene replacements in negative selection.

The *HXGPRT* selectable marker was precisely "cleaned" from two loci (Δ*ku80*::*HXGPRT* and Δ*uprt*::*HXGPRT*) in two of the four sequential gene replacement steps used to develop the triple mutant strain RHΔ*ku80*Δ*uprt*Δ*hxgprt* (Table 1). Strain RHΔ*ku80*Δ*hxgprt* provides an excellent genetic background for the efficient development of multiply manipulated strains using only the *HXGPRT* selectable marker.

Our results at the *CPSII* locus validate an efficient approach to complement a null phenotype (15) by direct gene replacement (of at least 24 kb) in strain RHΔ*ku80*Δ*hxgprt*. This experiment illustrates that the RHΔ*ku80*Δ*hxgprt* strain now enables more detailed studies on complementation and deciphering gene function(s) by directly targeting endogenous gene loci. This same knock-in double-crossover strategy can be used in the RHΔ*ku80*Δ*hxgprt* strain to directly and efficiently tag a protein (c-myc, HA, YFP/GFP/RFP, etc.) or to rapidly place a gene under regulatable protein (28) or transcriptional (48) expression.

Parasites from the phylum *Apicomplexa*, including *Plasmodium*, *Cryptosporidium*, *Babesia*, *Theileria*, and other related species (*Eimeria* and *Neospora*) possess many genes that share significant homology with *T. gondii* genes. A significant fraction of these genes are also selectively unique to the *Apicomplexa*, and these genes are often designated as a "hypothetical protein" (www.EuPathDB.org). Consequently, any gene knockout developed in the Δ*ku80* Δ*hxgprt* genetic background that reveals a biological phenotype can be used in complementation studies to replace the inserted *HXGPRT* marker (6TX negative selection) with the coding region of the complementing gene to clearly demonstrate a biological function for that "hypothetical" gene across the *Apicomplexa*.

Our results demonstrate that the *KU80* knockout genetic background is a valuable tool for higher-throughput development of nonreverting gene knockouts and gene replacements necessary for postgenome functional analysis of *T. gondii*. Our laboratory developed the Δ*ku80* Δ*hxgprt* genetic background to enable a global genetic dissection of the *Toxoplasma gondii* "nutriome," the collection of pathways and mechanisms controlling the acquisition of essential nutrients fueling obligate intracellular parasitism (2, 15, 17, 18, 20, 40). Fundamental questions remain to be answered as to how this clever obligate intracellular parasite has learned to successfully adapt to a large menu of host cells and hosts. The ability to now efficiently target gene replacements in the Δ*ku80* background is an important advancement for this model organism. Accelerated genetic dissection of protozoan parasite biology will more quickly lead to new treatments for significant parasitic diseases.

ACKNOWLEDGMENTS

We thank Leah M. Rommereim (Dartmouth) for critical reading of the manuscript. We thank Nicholas C. Callahan for construction of several pHXH plasmids used in this study. The work of the developers

of the *Toxoplasma gondii* Genome Resource at www.ToxoDB.org is gratefully acknowledged.

This work was partially supported by the NIH (AI073142, AI075931, and AI41930). This work was supported by the use of facilities that were provided from the Irradiation Shared Resource of the Dartmouth-Hitchcock Norris Cotton Cancer Center. ToxoDB, PlasmoDB, and EuPathDB are part of the NIH NIAID-funded Bioinformatics Resource Center.

REFERENCES

1. **Burton, P., D. J. McBride, J. M. Wilkes, J. D. Barry, and R. McCulloch.** 2007. Ku heterodimer-independent end joining in *Trypanosoma brucei* cell extracts relies upon sequence microhomology. Eukaryot. Cell **6:**1773–1781.
2. **Chaudhary, K., B. A. Fox, and D. J. Bzik.** 2007. *Toxoplasma gondii:* the model apicomplexan parasite: perspectives and methods. Elsevier, London, United Kingdom.
3. **Colot, H. V., G. Park, G. E. Turner, C. Ringelberg, C. M. Crew, L. Litvinkova, R. L. Weiss, K. A. Borkovich, and J. C. Dunlap.** 2006. A high-throughput gene knockout procedure for *Neurospora* reveals functions for multiple transcription factors. Proc. Natl. Acad. Sci. USA **103:**10352–10357.
4. **Conway, C., R. McCulloch, M. L. Ginger, N. P. Robinson, A. Browitt, and J. D. Barry.** 2002. Ku is important for telomere maintenance, but not for differential expression of telomeric VSG genes, in African trypanosomes. J. Biol. Chem. **277:**21269–21277.
5. **Cruz, A., and S. M. Beverley.** 1990. Gene replacement in parasitic protozoa. Nature **348:**171–173.
6. **Donald, R. G., D. Carter, B. Ullman, and D. S. Roos.** 1996. Insertional tagging, cloning, and expression of the *Toxoplasma gondii* hypoxanthine-xanthine-guanine phosphoribosyltransferase gene. Use as a selectable marker for stable transformation. J. Biol. Chem. **271:**14010–14019.
7. **Donald, R. G., and D. S. Roos.** 1998. Gene knock-outs and allelic replacements in *Toxoplasma gondii*: HXGPRT as a selectable marker for hit-and-run mutagenesis. Mol. Biochem. Parasitol. **91:**295–305.
8. **Donald, R. G., and D. S. Roos.** 1994. Homologous recombination and gene replacement at the dihydrofolate reductase-thymidylate synthase locus in *Toxoplasma gondii*. Mol. Biochem. Parasitol. **63:**243–253.
9. **Donald, R. G., and D. S. Roos.** 1995. Insertional mutagenesis and marker rescue in a protozoan parasite: cloning of the uracil phosphoribosyltransferase locus from *Toxoplasma gondii*. Proc. Natl. Acad. Sci. USA **92:**5749–5753.
10. **Donald, R. G., and D. S. Roos.** 1993. Stable molecular transformation of *Toxoplasma gondii*: a selectable dihydrofolate reductase-thymidylate synthase marker based on drug-resistance mutations in malaria. Proc. Natl. Acad. Sci. USA **90:**11703–11707.
11. **Dunlap, J. C., K. A. Borkovich, M. R. Henn, G. E. Turner, M. S. Sachs, N. L. Glass, K. McCluskey, M. Plamann, J. E. Galagan, B. W. Birren, R. L. Weiss, J. P. Townsend, J. J. Loros, M. A. Nelson, R. Lambreghts, H. V. Colot, G. Park, P. Collopy, C. Ringelberg, C. Crew, L. Litvinkova, D. DeCaprio, H. M. Hood, S. Curilla, M. Shi, M. Crawford, M. Koerhsen, P. Montgomery, L. Larson, M. Pearson, T. Kasuga, C. Tian, M. Basturkmen, L. Altamirano, and J. Xu.** 2007. Enabling a community to dissect an organism: overview of the *Neurospora* functional genomics project. Adv. Genet. **57:**49–96.
12. **Eid, J., and B. Sollner-Webb.** 1991. Stable integrative transformation of *Trypanosoma brucei* that occurs exclusively by homologous recombination. Proc. Natl. Acad. Sci. USA **88:**2118–2121.
13. **Fox, B. A., A. A. Belperron, and D. J. Bzik.** 2001. Negative selection of herpes simplex virus thymidine kinase in *Toxoplasma gondii*. Mol. Biochem. Parasitol. **116:**85–88.
14. **Fox, B. A., A. A. Belperron, and D. J. Bzik.** 1999. Stable transformation of *Toxoplasma gondii* based on a pyrimethamine resistant trifunctional dihydrofolate reductase-cytosine deaminase-thymidylate synthase gene that confers sensitivity to 5-fluorocytosine. Mol. Biochem. Parasitol. **98:**93–103.
15. **Fox, B. A., and D. J. Bzik.** 2002. De novo pyrimidine biosynthesis is required for virulence of *Toxoplasma gondii*. Nature **415:**926–929.
16. **Fox, B. A., and D. J. Bzik.** 2003. Organisation and sequence determination of glutamine-dependent carbamoyl phosphate synthetase II in *Toxoplasma gondii*. Int. J. Parasitol. **33:**89–96.
17. **Fox, B. A., K. Chaudhary, and D. J. Bzik.** 2007. *Toxoplasma*: molecular and cellular biology. Horizon Bioscience, Norwich, United Kingdom.
18. **Fox, B. A., J. P. Gigley, and D. J. Bzik.** 2004. *Toxoplasma gondii* lacks the enzymes required for de novo arginine biosynthesis and arginine starvation triggers cyst formation. Int. J. Parasitol. **34:**323–331.
19. **Fox, B. A., W. B. Li, M. Tanaka, J. Inselburg, and D. J. Bzik.** 1993. Molecular characterization of the largest subunit of *Plasmodium falciparum* RNA polymerase I. Mol. Biochem. Parasitol. **61:**37–48.
20. **Fox, B. A., J. G. Ristuccia, and D. J. Bzik.** 2008. Genetic dissection of essential indels and domains in carbamoyl phosphate synthetase II of *Toxoplasma gondii*. Int. J. Parasitol. **39:**533–539
21. **Gardner, M. J., N. Hall, E. Fung, O. White, M. Berriman, R. W. Hyman, J. M. Carlton, A. Pain, K. E. Nelson, S. Bowman, I. T. Paulsen, K. James, J. A. Eisen, K. Rutherford, S. L. Salzberg, A. Craig, S. Kyes, M. S. Chan, V. Nene, S. J. Shallom, B. Suh, J. Peterson, S. Angiuoli, M. Pertea, J. Allen, J. Selengut, D. Haft, M. W. Mather, A. B. Vaidya, D. M. Martin, A. H. Fairlamb, M. J. Fraunholz, D. S. Roos, S. A. Ralph, G. I. McFadden, L. M. Cummings, G. M. Subramanian, C. Mungall, J. C. Venter, D. J. Carucci, S. L. Hoffman, C. Newbold, R. W. Davis, C. M. Fraser, and B. Barrell.** 2002. Genome sequence of the human malaria parasite *Plasmodium falciparum*. Nature **419:**498–511.
22. **Giaever, G., A. M. Chu, L. Ni, C. Connelly, L. Riles, S. Veronneau, S. Dow, A. Lucau-Danila, K. Anderson, B. Andre, A. P. Arkin, A. Astromoff, M. El-Bakkoury, R. Bangham, R. Benito, S. Brachat, S. Campanaro, M. Curtiss, K. Davis, A. Deutschbauer, K. D. Entian, P. Flaherty, F. Foury, D. J. Garfinkel, M. Gerstein, D. Gotte, U. Guldener, J. H. Hegemann, S. Hempel, Z. Herman, D. F. Jaramillo, D. E. Kelly, S. L. Kelly, P. Kotter, D. LaBonte, D. C. Lamb, N. Lan, H. Liang, H. Liao, L. Liu, C. Luo, M. Lussier, R. Mao, P. Menard, S. L. Ooi, J. L. Revuelta, C. J. Roberts, M. Rose, P. Ross-Macdonald, B. Scherens, G. Schimmack, B. Shafer, D. D. Shoemaker, S. Sookhai-Mahadeo, R. K. Storms, J. N. Strathern, G. Valle, M. Voet, G. Volckaert, C. Y. Wang, T. R. Ward, J. Wilhelmy, E. A. Winzeler, Y. Yang, G. Yen, E. Youngman, K. Yu, H. Bussey, J. D. Boeke, M. Snyder, P. Philippsen, R. W. Davis, and M. Johnston.** 2002. Functional profiling of the *Saccharomyces cerevisiae* genome. Nature **418:**387–391.
23. **Gilbert, L. A., S. Ravindran, J. M. Turetzky, J. C. Boothroyd, and P. J. Bradley.** 2007. *Toxoplasma gondii* targets a protein phosphatase 2C to the nuclei of infected host cells. Eukaryot. Cell **6:**73–83.
24. **Glover, L., R. McCulloch, and D. Horn.** 2008. Sequence homology and microhomology dominate chromosomal double-strand break repair in African trypanosomes. Nucleic Acids Res. **36:**2608–2618.
25. **Goins, C. L., K. J. Gerik, and J. K. Lodge.** 2006. Improvements to gene deletion in the fungal pathogen *Cryptococcus neoformans*: absence of Ku proteins increases homologous recombination, and co-transformation of independent DNA molecules allows rapid complementation of deletion phenotypes. Fungal Genet. Biol. **43:**531–544.
26. **Gubbels, M. J., M. Lehmann, M. Muthalagi, M. E. Jerome, C. F. Brooks, T. Szatanek, J. Flynn, B. Parrot, J. Radke, B. Striepen, and M. W. White.** 2008. Forward genetic analysis of the apicomplexan cell division cycle in *Toxoplasma gondii*. PLoS Pathog. **4:**e36.
27. **Haber, J. E.** 2000. Partners and pathways repairing a double-strand break. Trends Genet. **16:**259–264.
28. **Herm-Gotz, A., C. Agop-Nersesian, S. Munter, J. S. Grimley, T. J. Wandless, F. Frischknecht, and M. Meissner.** 2007. Rapid control of protein level in the apicomplexan *Toxoplasma gondii*. Nat. Methods **4:**1003–1005.
29. **Ishibashi, K., K. Suzuki, Y. Ando, C. Takakura, and H. Inoue.** 2006. Nonhomologous chromosomal integration of foreign DNA is completely dependent on MUS-53 (human Lig4 homolog) in *Neurospora*. Proc. Natl. Acad. Sci. USA **103:**14871–14876.
30. **Janzen, C. J., F. Lander, O. Dreesen, and G. A. Cross.** 2004. Telomere length regulation and transcriptional silencing in KU80-deficient *Trypanosoma brucei*. Nucleic Acids Res. **32:**6575–6584.
31. **Kim, K., D. Soldati, and J. C. Boothroyd.** 1993. Gene replacement in *Toxoplasma gondii* with chloramphenicol acetyltransferase as selectable marker. Science **262:**911–914.
32. **Kim, K., and L. M. Weiss.** 2004. *Toxoplasma gondii*: the model apicomplexan. Int. J. Parasitol. **34:**423–432.
33. **Kim, K., and L. M. Weiss.** 2008. *Toxoplasma:* the next 100 years. Microbes Infect. **10:**978–984.
34. **Kirisits, M. J., E. Mui, and R. McLeod.** 2000. Measurement of the efficacy of vaccines and antimicrobial therapy against infection with *Toxoplasma gondii*. Int. J. Parasitol. **30:**149–155.
35. **Kooistra, R., P. J. Hooykaas, and H. Y. Steensma.** 2004. Efficient gene targeting in *Kluyveromyces lactis*. Yeast **21:**781–792.
36. **Mazumdar, J., E. H. Wilson, K. Masek, C. A. Hunter, and B. Striepen.** 2006. Apicoplast fatty acid synthesis is essential for organelle biogenesis and parasite survival in *Toxoplasma gondii*. Proc. Natl. Acad. Sci. USA **103:**13192–13197.
37. **Mercier, C., J. F. Dubremetz, B. Rauscher, L. Lecordier, L. D. Sibley, and M. F. Cesbron-Delauw.** 2002. Biogenesis of nanotubular network in *Toxoplasma* parasitophorous vacuole induced by parasite proteins. Mol. Biol. Cell **13:**2397–2409.
38. **Messina, M., I. Niesman, C. Mercier, and L. D. Sibley.** 1995. Stable DNA transformation of *Toxoplasma gondii* using phleomycin selection. Gene **165:**213–217.
39. **Meyer, V., M. Arentshorst, A. El-Ghezal, A. C. Drews, R. Kooistra, C. A. van den Hondel, and A. F. Ram.** 2007. Highly efficient gene targeting in the *Aspergillus niger* kusA mutant. J. Biotechnol. **128:**770–775.
40. **Ngo, H. M., E. O. Ngo, D. J. Bzik, and K. A. Joiner.** 2000. *Toxoplasma gondii*: are host cell adenosine nucleotides a direct source for purine salvage? Exp. Parasitol. **95:**148–153.
41. **Ninomiya, Y., K. Suzuki, C. Ishii, and H. Inoue.** 2004. Highly efficient gene replacements in *Neurospora* strains deficient for nonhomologous end-joining. Proc. Natl. Acad. Sci. USA **101:**12248–12253.
42. **Pfefferkorn, E. R.** 1978. *Toxoplasma gondii*: the enzymic defect of a mutant resistant to 5-fluorodeoxyuridine. Exp. Parasitol. **44:**26–35.
43. **Pfefferkorn, E. R., D. J. Bzik, and C. P. Honsinger.** 2001. *Toxoplasma gondii*:

mechanism of the parasitostatic action of 6-thioxanthine. Exp. Parasitol. **99:**235–243.
44. **Pfefferkorn, E. R., and L. C. Pfefferkorn.** 1976. *Toxoplasma gondii*: isolation and preliminary characterization of temperature-sensitive mutants. Exp. Parasitol. **39:**365–376.
45. **Roos, D. S., W. J. Sullivan, B. Striepen, W. Bohne, and R. G. Donald.** 1997. Tagging genes and trapping promoters in *Toxoplasma gondii* by insertional mutagenesis. Methods **13:**112–122.
46. **Sabin, A. B.** 1941. *Toxoplasmic* encephalitis in children. JAMA **116:**801–807.
47. **Shaw, M. K., D. S. Roos, and L. G. Tilney.** 2001. DNA replication and daughter cell budding are not tightly linked in the protozoan parasite *Toxoplasma gondii*. Microbes Infect. **3:**351–362.
48. **van Poppel, N. F., J. Welagen, R. F. Duisters, A. N. Vermeulen, and D. Schaap.** 2006. Tight control of transcription in *Toxoplasma gondii* using an alternative tet repressor. Int. J. Parasitol. **36:**443–452.
49. **Walker, J. R., R. A. Corpina, and J. Goldberg.** 2001. Structure of the Ku heterodimer bound to DNA and its implications for double-strand break repair. Nature **412:**607–614.
50. **Wu, D., L. M. Topper, and T. E. Wilson.** 2008. Recruitment and dissociation of nonhomologous end joining proteins at a DNA double-strand break in *Saccharomyces cerevisiae*. Genetics **178:**1237–1249.
51. **Wu, Y., L. A. Kirkman, and T. E. Wellems.** 1996. Transformation of *Plasmodium falciparum* malaria parasites by homologous integration of plasmids that confer resistance to pyrimethamine. Proc. Natl. Acad. Sci. USA **93:** 1130–1140.